# ECW/EBW Heating and Current Drive Experiment Results and Prospects for CW Operation in QUEST*)

Hiroshi IDEI, Hideki ZUSHI, Kazuaki HANADA, Evgeniya KALINNIKOVA[1)], Kazuo NAKAMURA, Akihide FUJISAWA, Yoshihiko NAGASHIMA, Makoto HASEGAWA, Keisuke MATSUOKA, Tsuyoshi KARIYA[2)], Tsuyoshi IMAI[2)], Ryutaro MINAMI[2)], Naoaki YOSHIDA, Mizuki SAKAMOTO[2)], Hideo WATANABE, Kazutoshi TOKUNAGA, Akira EJIRI[3)], Masatsugu SAKAGUCHI[1)], Masaki ISHIGURO[1)], Saya TASHIMA[1)], Atsushi FUKUYAMA[4)], Hiroe IGAMI[5)], Shin KUBO[5)], Mitsutaka ISOBE[5)], Kenichi NAGAOKA[5)], Hideya NAKANISHI[5)], Nobuhiro NISHINO[6)], Shoji KAWASAKI, Hisatoshi NAKASHIMA, Aki HIGASHIJIMA, Yuichi TAKASE[3)], Takashi MAEKAWA[7)], Osamu MITARAI[8)], Mitsuru KIKUCHI[9)] and Kazuo TOI[5)]

*Research Institute for Fusion Science, Kasuga 816-8580, Japan*
[1)]*Interdisciplinary Graduate School of Engineering Science, Kyushu University, Kasuga 816-8580, Japan*
[2)]*Plasma Research Center, Tsukuba University, Tsukuba 305-8577, Japan*
[3)]*Department of Complexity Science and Engineering, University of Tokyo, Kashiwa 277-8561, Japan*
[4)]*Department of Nuclear Engineering, Kyoto University, Kyoto 606-8501, Japan*
[5)]*National Institute for Fusion Science, Toki 509-5292, Japan*
[6)]*Mechanical System Engineering, Hiroshima University, Hiroshima 739-8527, Japan*
[7)]*Graduate School of Energy Science, Kyoto University, Kyoto 606-8501, Japan*
[8)]*Institute of Industrial Science and Technology Research, Tokai University, Kumamoto 862-8652, Japan*
[9)]*Japan Atomic Energy Agency, Naka 311-0193, Japan*

(Received 12 December 2011 / Accepted 11 May 2012)

A CW phased-array antenna system for electron cyclotron/Bernstein wave heating and current drive (ECWH/CD, EBWH/CD) experiments was developed in the QUEST. The antenna was designed to excite an elliptically polarized pure O-mode wave in oblique injection for the O-X-B mode conversion scenario, and its good performance was confirmed at a high power level. Long pulse discharges with a plasma current of 10 kA and 15 kA were non-inductively attained for 37 s and 20 s, respectively, with only radio frequency (RF) power. Divertor configurations were also obtained in the RF-sustained plasmas. A new operational window for sustained plasma current was observed in the high-density plasma with a higher RF incident power. Two new heating and current drive systems with an 8.56 GHz klystron and a 28 GHz gyrotron are being prepared to conduct CW EBWH/CD experiments in the high-density plasma.



Keywords: electron Bernstein wave, spherical tokamak, QUEST, phased-array antenna

DOI: 10.1585/pfr.7.2402112

## 1. Introduction

The Q-shu University Experiments with Steady-State Spherical Tokamak (QUEST) was proposed at Kyushu University, and the QUEST device has been constructed [1]. Spherical tokamaks (STs) can attain a higher $\beta$ than conventional tokamaks. The ultimate goal of the QUEST project is steady-state operation with relatively high beta (<10%) in the ST configuration under controlled plasma wall interactions. For steady-state tokamak operation, a plasma current drive method should be established. Electron Bernstein wave heating and current drive (EBWH/CD) is an attractive candidate for sustaining a steady-state ST plasma. In ST experiments, the plasma frequency may become larger than the electron cyclotron frequency in the operating density range because of the low magnetic field, and electron cyclotron waves cannot propagate into the plasma beyond the cutoff. EBWH/CD experiments require mode conversion processes from the electron cyclotron (electromagnetic) waves to the electron Bernstein (electrostatic) wave.

In O-X-B mode conversion, an obliquely incident electromagnetic O-mode wave that reaches the cutoff is converted into an X-mode wave and propagates to the upper hybrid resonance layer. It is then converted to an electrostatic Bernstein- (B-) mode wave. A ray trajectory in an optimum case where the O-mode wave is obliquely injected with an appropriate parallel refractive index $N_{//}$ was

*author's e-mail: idei@triam.kyushu-u.ac.jp*
*) This article is based on the invited presentation at the 21st International Toki Conference (ITC21).

analyzed using the TASK/WR ray-tracing code [2], and the deposition profile was evaluated. The generated current profile was also analyzed using the TASK/FP Fokker-Planck code from the local wave electric fields calculated by the TASK/WR code [3]. Multiple ray propagations were analyzed with the $N_{//}$ spectrum, including non-optimal cases, taking into account the tunneling effect through the evanescent layer beyond the cutoff [4]. The propagation and absorption of each ray in the multiple-ray analysis was calculated individually, and the total absorption was evaluated as a superposition of all the rays' absorption. In O-X-B mode conversion experiments, the launching angle and elliptical polarization state should be controlled to achieve high-efficiency mode conversion into the B-mode wave. A phased-array antenna (PAA) system that enabled us to control the launching angle and elliptical polarization state was proposed [5] for the EBWH/CD experiments in the QUEST. The PAA structure was modified from the prototype design to reduce the side lobes in the PAA radiation field [6], and a CW PAA with forced cooling water channels was developed. A low-power test of the CW antenna confirmed its good performance with small side lobes [7]. The CW PAA's performance was recently evaluated in the QUEST vacuum vessel at a high power level. RF startup and sustainment experiments using the CW PAA system have progressed to expand the obtained plasma current region, but their densities were still lower than the cutoff density. A new operational window for sustained plasma current was observed in the high-density plasma at the higher RF incident power.

This paper is organized as follows. Section 2 describes the high-power test of the CW PAA system in the QUEST device. Recent progress on the heating and current drive experiments is presented in Section 3. A new heating and current drive system with an 8.56 GHz klystron is introduced in Section 4. Section 5 describes a new heating system with a 28 GHz gyrotron. Finally, a summary is given in Section 6.

## 2. High-Power Test of PAA System in the QUEST Device

A [4×2] CW antenna system with eight waveguide ports was designed to reduce the side lobes observed in the prototype antenna. The waveguide size and wall thickness of the PAA waveguide port were smaller in the CW PAAs than in the prototype. A strong forced cooling structure was designed to remove the heat load at the interface regions of the PAA waveguide ports. The CW antenna performance was evaluated at Kyushu University's low-power facilities. An 8.2 GHz system with eight klystrons has been used for ECW/EBW experiments in the QUEST. The system was prepared for the lower hybrid current drive (LHCD) experiments in our earlier TRIAM-1M tokamak [8]. Each klystron generated a nominal 25 kW oscillating power, and its output was divided into two fundamental waveguide transmission lines with a magic tee. Sixteen waveguide transmission lines and a grill antenna were used to conduct the LHCD experiments in the TRIAM-1M tokamak. To make a phased array of the LHCD grill antenna, 3 dB hybrid phase shifters were installed on the transmission lines. The phase shifters were also available for phased array adjustment in the CW PAA system. The adjusted phase array was measured at the directional couplers of the developed PAA system in vacuum. The phase relationship among the waveguide ports was calibrated in the low-power test in which the PAA performance was evaluated. Because the total transmission system including the developed PAA was complicated, the phase relationship or the fields radiated from the PAA should be confirmed at a high power level in the QUEST device with all the transmission lines, including the CW PAA system. The 8.2 GHz klystron amplified the exciter input to a high power output. The amplifier gain was about 43 dB. A rather high exciter level (~1 W) was required to generate a nominal 25 kW output from the klystron. Because the exciter system exhibited thermal frequency drift, a Peltier module was installed to maintain the exciter temperature, however, a small frequency drift was still observed. Excellent frequency stability is generally required for precise phase measurements. In the low-power test, the frequencies of two synthesizers used to launch a test beam and feed the local oscillator power at the receiving mixers were locked with a stable 10 MHz clock. Figure 1 shows a schematic of the measurement system used in the high-power test of the PAA. A single side band (SSB) up-converter was used for heterodyne detection. In this heterodyne system, the intermediate frequency (IF) detected at the mixers never changed even if the operating frequency of the klystron changed because of frequency drift in the exciter. The IF frequency was locked for precise phase measurements in the high-power test. To avoid damage to the receiving mixer, a large attenuation was prepared, and the pulse duration was limited to 3 ms. A reference

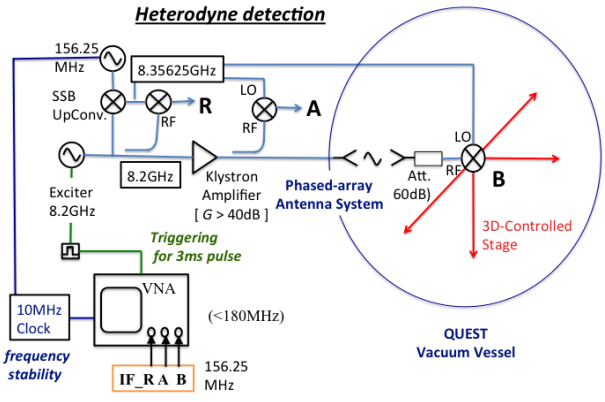


Fig. 1 Schematic of field measurement system of developed [4×2] CW phased-array antenna with a high power level in the QUEST device.

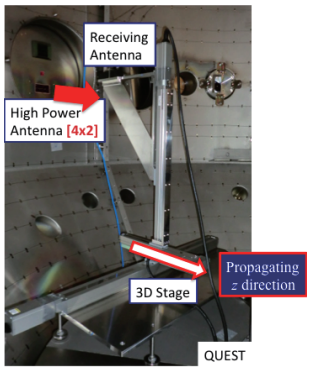


Fig. 2 Experimental setup of high-power test of the [4×2] CW phased-array antenna in the QUEST device.

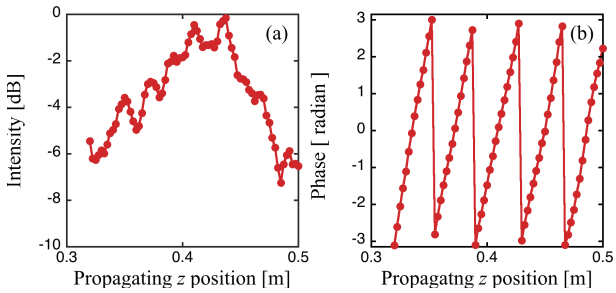


Fig. 3 (a) Intensity and (b) phase profiles along the propagating $z$ direction when one of the [4×2] waveguide ports is excited in the high-power test.

IF signal was also measured with a vector network analyzer to determine the amplitude ratio and phase difference for the receiving side after propagation from the PAA. The dynamic range of the amplitude measurement was 90 dB. Figure 2 shows the experimental setup of the PAA high-power test in the QUEST device. The PC-controlled three-dimensional scanner was set to measure the field distributions radiating from the PAA in the QUEST vacuum vessel. The setting error of the scanner position was less than 0.1 mm. The antenna position was controlled within 1/300th of the wavelength. The QUEST vacuum vessel may work as a large oversized cavity in the case of RF injection to the device. The major and minor (plasma) radii of the QUEST device are 0.64 m and 0.16 m, respectively. The vacuum vessel was quite oversized for the wavelength (~ 0.037 m) of 8.2 GHz. The standing wave components were sometimes dominant in the cavity condition, preventing us from creating the phase array. First, the field radiated by the PAA was measured along the propagating $z$ direction to determine whether the propagating wave-field component was properly measured. Figure 3 shows the intensity and phase profiles along the propagating $z$ direction when one of the [4×2] waveguide ports was excited. The proper $kz$ phase evolution was measured along the propagation direction, where $k$ was the 8.2 GHz wavenumber. The intensity profile exhibited complicated fine structures caused

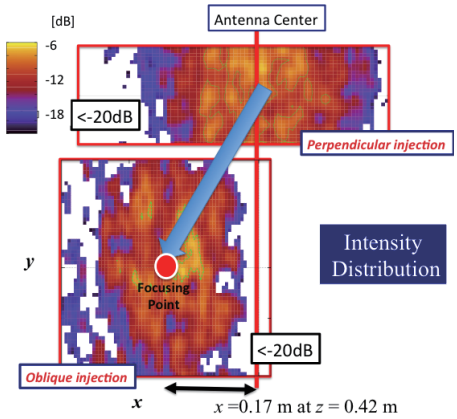


Fig. 4 Intensity contour plots in the $x-y$ plane perpendicular to the propagating $z$ direction for perpendicular and oblique injection.

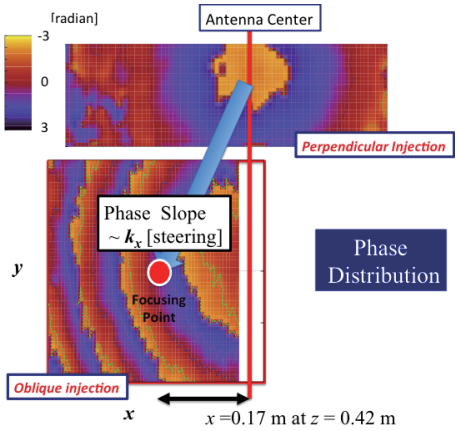


Fig. 5 Phase contour plots in the $x-y$ plane perpendicular to the propagating $z$ direction for perpendicular and oblique injection.

by phase interference along the $kz$ evolution, including a global interference effect in the oversized cavity condition. Figure 4 shows intensity contour plots in the $x-y$ plane perpendicular to the propagating $z$ direction for perpendicular and oblique injection. Although the profiles were complicated because of the interference effect, the beam was focused at the center of the antenna in perpendicular injection and was steered in the $x$ direction at a focusing point ( [$x$, $z$] = [0.17 m, 0.42 m] ) in oblique injection. In oblique injection, the intensity in front of the antenna center was less than the intensity of the steered beam center by 20 dB or more. Figure 5 shows phase contour plots in the $x-y$ plane perpendicular to the propagating $z$ direction for perpendicular and oblique injection. In perpendicular injection, the parabolic phase profile showed a focused beam expanding along the propagation direction. In oblique injection, a gradient in the phase profiles was observed in the $x$ direction at the focusing point, indicating that the beam was steered in the $x$ direction. The $x$ derivative of the phase profile expressed the $x$ component of the wavenumber, $k_x$. Figure 6

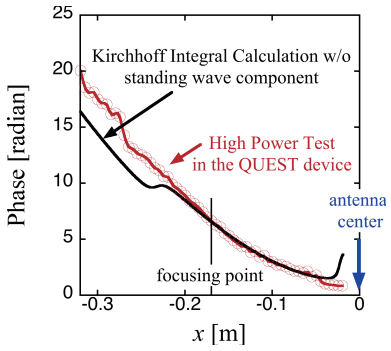


Fig. 6 Phase profiles in the $x$ direction at $y = 0$ measured in the high-power test and calculated by a developed Kirchhoff integral code without considering the standing wave effect.

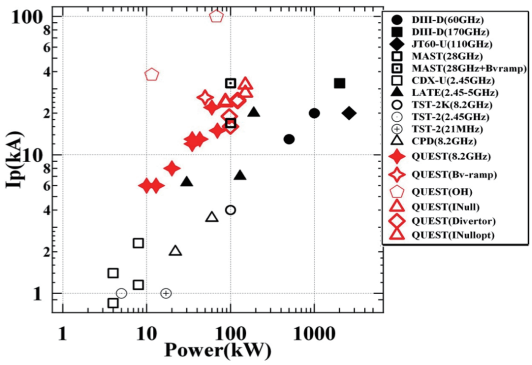


Fig. 7 Recent progress in obtained plasma currents for various incident RF powers. Red symbols represent QUEST results.

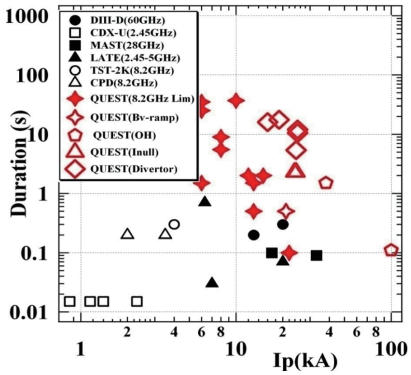


Fig. 8 Recent progress in obtained pulse durations for various plasma currents. Red symbols represent QUEST results.

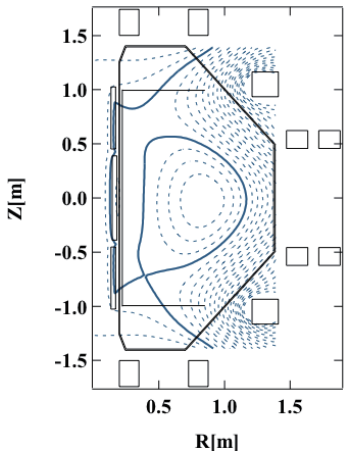


Fig. 9 Reconstructed magnetic fluxes in the divertor configuration with a plasma current of 15 kA.

shows phase profiles in the $x$ direction at $y = 0$ measured in the high-power test and calculated by a developed Kirchhoff integral code without considering the standing wave effect. The measured phase gradient, or $k_x$, coincided well with that calculated using the Kirchhoff integral code at the focusing point, whereas the measured profile deviated from the calculated one owing to the standing wave component in regions where the intensity was small, such as the center of the antenna. The high-power test confirmed that the developed PAA has good focusing and steering properties.

# 3. Recent Progress in Heating and Current Drive Experiments in QUEST

## 3.1 Long pulse discharges in limiter and divertor configurations

The plasma currents obtained in the QUEST are plotted as a function of the incident RF power in Fig. 7. Figure 8 shows the obtained pulse duration for each plasma current. Long pulse discharges at plasma currents of 10 kA and 15 kA were attained for 37 s and 20 s, respectively, in the limiter configuration. A hot spot appeared in the outer limiter, and metal contamination was observed as well as recycling enhancement with the increased $H_\alpha$ intensity of the long pulse discharges. Non-inductive divertor experiments were conducted with poloidal field coil control. Figure 9 shows the reconstructed magnetic fluxes in the divertor configuration with a plasma current of 15 kA. The elongation, triangularity, and aspect ratio were 1.53, 0.41, and 1.98, respectively. To obtain a single-null configuration, the vertical plasma position was controlled to be 0.04 m lower for the midplane of the QUEST device. The single-null divertor configuration with a high plasma current (<~25 kA) was also attained in the 17 s plasma sustainment.

The obtained density was typically low ($\sim 2 \times 10^{17}\,\mathrm{m}^{-3}$) compared to the O-mode cutoff density ($\sim 8 \times 10^{17}\,\mathrm{m}^{-3}$) in these experiments. Effective EBWH/CD experiments in the O-X-B mode conversion scenario were not anticipated in the low-density plasma with the developed PAA. The RF powers plotted in Fig. 7 were entirely injected using two 8.2 GHz systems with and without PAA operation. The hard X-ray intensity from

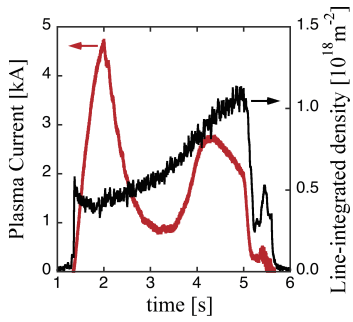


Fig. 10 Time evolutions of plasma current and density obtained in high-density discharge.

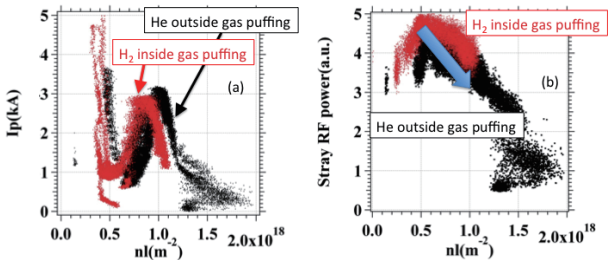


Fig. 11 Obtained (a) plasma current and (b) stray radiation component of the incident RF power for line-integrated density in hydrogen and helium discharges.

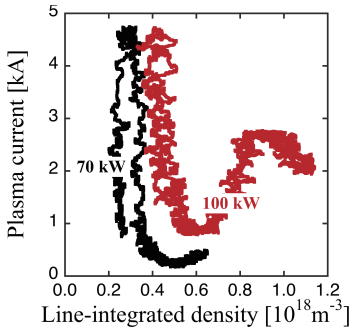


Fig. 12 Obtained plasma current with respect to the line-integrated density at 70 and 100 kW incident power injection in helium discharges.

current-carrying electrons accelerated by the incident RF power was ramped up in the energy range of 10~30 keV, following the plasma current evolution. An asymmetric confinement structure of high-energy electrons on the parallel velocity in velocity space may explain the generated current. The vertical magnetic field $B_V$ along the toroidal field $B_T$ is required to start up the plasma current by RF injection alone. Specific electrons can be confined well if the vertical motion due to the toroidal drift $v_{dT}$ is cancelled by the vertical component of the parallel velocity due to the magnetic field pitch angle $v_{//}(B_V/B_T)$ [9]. These confined electrons can contribute to the plasma current of the RF-sustained plasma. The direction of plasma current depends on the direction of $B_V$ because only the co-moving electrons for which $v_{//}(B_V/B_T)$ is opposite to $v_{dT}$ can be confined well. In addition, banana orbits are possible even on open field lines. Thus, the confined trapped electrons also contribute to current generation owing to the precession in the toroidal direction.

### 3.2 High-density operation

To study the EBWH/CD effect, a high-density plasma should first be produced and sustained in the ECWH/CD experiments. High-density operation was conducted in the inboard null configuration [10]. The divertor configurations formed single- and double-null points upper and/or lower for the midplane in the QUEST device. In the inboard null configuration, a null point appeared on the high field side of the QUEST device. The high-energy electrons could be confined by the strong positive $n$-index field. Figure 10 shows the time evolution of the plasma current and density obtained in this configuration. A series of gas puffs was applied to obtain the high-density plasma. The plasma current decreased initially, but, remarkably, it was observed again in the higher-density plasma. In addition to a hydrogen discharge, helium and neon discharge experiments were conducted to obtain a high-density plasma in the inboard null configuration. Figure 11 shows the obtained plasma currents and the stray radiation components of the incident RF power for the line-integrated density in the hydrogen and helium discharges. A new operational window for sustained plasma current was more clearly observed in the helium discharge experiments. The stray radiation decreased as the density increased in both the helium and hydrogen discharges, indicating that most of the incident power was absorbed by the high-density plasma. Figure 12 shows the obtained plasma current with respect to the line-integrated density at 70 and 100 kW power injection in the helium discharges. The high-density window was not achieved at the lower RF incident power.

## 4. New High- Power and Frequency Systems

### 4.1 8.56 GHz High-power klystron system

A higher incident power was required to obtain the new operational window with a significant plasma current in the high-density plasma. A new high-power 8.56 GHz klystron (VKX-7864B1) manufactured by Communications & Power Industries was prepared for the EBWH/CD experiments in the QUEST. Figure 13 shows photographs of the new klystron. Its nominal oscillating power is 250 kW in CW operation, and its operational beam voltage and current are -52 kV and 13 A, respectively. This klystron will be operated using a gyrotron power supply prepared for the ECWH/CD experiments in the TRIAM-1M tokamak. The maximum beam voltage and current of the gyrotron power supply are -75 kV and 25 A. Regulator tube and crowbar systems were prepared to protect the

Fig. 13 Photographs of new 8.56 GHz klystron (Communications & Power Industries: VKX-7864B1).

gyrotron. The protection system can cut the high voltage applied to the gyrotron within 10 μs of the detection of an overcurrent due to an arcing event inside the gyrotron. The energy entering the gyrotron owing to arcing should be less than 10 J. A lower incoming energy of 5 J is required for klystron operation. A protective resister system was also prepared to limit the incoming energy to 5 J. Some waveguide components such as an isolator, an arc sensor, and a directional coupler were prepared. An exciter system composed of a synthesizer and a high-power amplifier is being prepared. The high-power klystron system will be operated with the modified gyrotron power supply in summer 2012.

## 4.2 28 GHz gyrotron system

The O-mode cutoff density increases as the square of the operating RF frequency. If a high-frequency power source is available for the ECWH/CD experiments, the accessible density in the experiments increases. Figure 14 shows the fundamental and second electron cyclotron resonance frequencies, $f_{ce}$ and $2f_{ce}$, at $B_T$ = 0.25 T, and the O-mode cutoff frequencies $f_{pe}$ for various density profiles. The $2f_{ce}$ at 28 GHz was located at the high field side, as was $f_{ce}$ at 8.2/8.56 GHz near the plasma center, as shown in Fig. 14. The O-mode cutoff density is $1 \times 10^{19}$ m$^{-3}$ at 28 GHz. The incident 28 GHz ECW can propagate into the plasma beyond the cutoff density for 8.2/8.56 GHz ($> 8 \times 10^{17}$ m$^{-3}$). EBWH/CD experiments are planned that will use two frequency range sources of 28 GHz and 8.2/8.56 GHz. The plasma will initially be produced by the 8.2/8.56 GHz system, and then the density will be ramped up with the 28 GHz system. The 8.2/8.56 GHz EBWH/CD experiments can be conducted in the overdense plasma sustained by the high-frequency 28 GHz system. Kyushu University, Tsukuba University and the National Institute for Fusion Science (NIFS) have begun bi-directional collaborative research. A 77 GHz CW gyrotron has been successfully developed for the Large Helical Device experiments by collaborative research between Tsukuba University and the NIFS. The research program at Tsukuba University has developed a 28 GHz CW gyrotron. It will be used for the

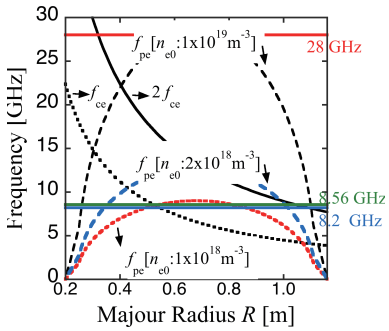


Fig. 14 Fundamental and second electron cyclotron resonance frequencies $f_{ce}$ and $2f_{ce}$ at 0.25 T in CW operation, and O-mode cutoff frequencies $f_{pe}$ for various density profiles. The density profiles are assumed to be parabolic with different central densities $n_{e0}$ of $0.1/0.2/1.0 \times 10^{19}$ m$^{-3}$.

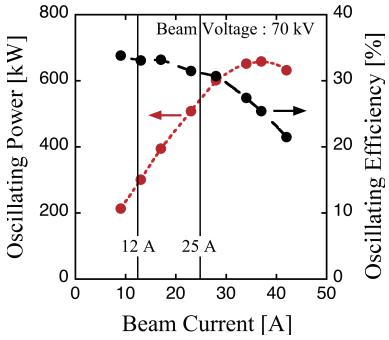


Fig. 15 Oscillating output power and efficiency at beam voltage of -70 kV as a function of the beam current for the 28 GHz gyrotron. Power supply current limits of 12 A and 25 A appeared for operation scenarios with and without the 8.56 GHz klystron in parallel, respectively.

EBWH/CD experiments with the gyrotron power supply at Kyushu University. The 28 GHz gyrotron was operated at a beam voltage of -80 kV to obtain a maximum oscillating power level of 1 MW at Tsukuba University. The maximum beam voltage was -75 kV in the Kyushu University power supply for the gyrotron. The operating parameter region of the 28 GHz gyrotron was surveyed in order to operate it with a lower beam voltage at Kyushu University. Figure 15 shows the oscillating output power and efficiency at a beam voltage of -70 kV as a function of the beam current. The maximum beam current for the Kyushu University power supply was limited to 25 A. A power level of 500~600 kW was available within the operating limits of the power supply. The oscillating efficiencies will be improved in the operating region at Kyushu University. The Tsukuba 28 GHz gyrotron was operated with a triode magnetron injection gun (MIG), whereas a 170 GHz gyrotron for the TRIAM-1M tokamak was operated with a diode MIG. The maximum anode voltage was 42.5 kV for operation with the -70 kV beam voltage. A conventional high-voltage power supply of 50 kV was pre-

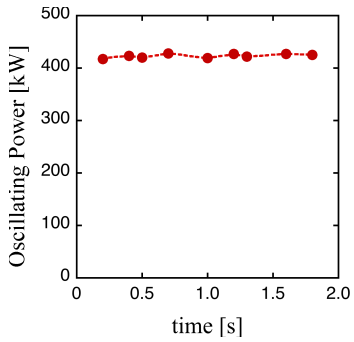


Fig. 16 Oscillating output power for long pulse operation of the 28 GHz gyrotron.

pared to control the anode voltage. A high-speed, high-voltage CW switch system that integrates multiple stages of MOSFETs connected in series is being prepared to turn the anode voltage on and off and to cut the voltage upon overcurrent detection. An overcurrent detection system for the anode current and a gyrotron tank with insulators for the anode and body electrodes were prepared in addition to the gyrotron system at Kyushu University.

If the 28 GHz gyrotron will be operated in parallel with the 8.56 GHz klystron using the same high-voltage power supply, collector potential depressed (CPD) operation should be considered. In CPD operation, the total voltage accelerating an electron beam in the gyrotron is the voltage difference between the cathode and the body. The withstand voltage between the body and collector electrodes was evaluated at Tsukuba University, and its maximum value was 17~18 kV. The electric potential at the collector electrode, which connects to the ground through a beam-current-monitoring resistance, was essentially zero. The gyrotron can be operated with a cathode voltage of -52 kV and a body voltage of +17 to +18 kV in CPD operation together with the 8.56 GHz klystron. The total voltage accelerating the electron beam becomes 69~70 [52+ (17~18)] kV. An additional body power supply at the 20 kV level will be required for CPD operation. The total beam current should be less than 25 A on the Kyushu University power supply. Because the operating current of the 8.56 GHz klystron is 13 A, the gyrotron may be operated in parallel at a beam current of 12 A. The oscillating power level of the gyrotron will be limited to 250~300 kW. Long pulse operation of the 28 GHz gyrotron was demonstrated at a rather low power level at Tsukuba University. Figure 16 shows the gyrotron oscillating power for long pulse operation. The power level of 400 kW was available for 1.8 s. In principle, the 28 GHz gyrotron can be operated continuously in parallel with the 8.56 GHz klystron.

## 5. Summary

The performance of the developed [4 × 2] CW antenna was tested at a high power level in the QUEST device. A heterodyne detection system with frequency-locking IF signals was used in the high-power test. The beam was properly steered to the focusing point in oblique injection, taking the gradient of the phase profile there. Long pulse discharges with plasma currents of 10 kA and 15 kA were attained for 37 s and 20 s in the limiter configurations, respectively. The single-null divertor configuration was obtained with the 15 kA plasma current. The elongation, triangularity, and aspect ratio were 1.53, 0.41, and 1.98, respectively. The divertor configuration with a high plasma current (<~25 kA) was also achieved during 17 s plasma sustainment. High-density operation was conducted in helium and neon discharges as well as a hydrogen discharge. A new operational window for sustained plasma current was observed in the high-density plasma at the higher RF incident power. High-power/frequency systems for use in EBWH/CD experiments in high-density plasma were considered in the QUEST. The 8.56 GHz CW klystron and its related components were prepared for the high-power experiments. The operating parameter region of the 28 GHz gyrotron was surveyed in order to operate it within the limits of the Kyushu University power supply. CPD operation of the 28 GHz gyrotron was considered for joint operation with the 8.56 GHz klystron. The gyrotron can be operated at power levels of 500~600 kW and 250~300 kW without and with the 8.56 GHz klystron operation in parallel, respectively. A long pulse of 1.8 s was attained at a power level of 400 kW. The required anode voltage power supply, a gyrotron tank, and an overcurrent detection system were prepared for operation at Kyushu University.

## Acknowledgments

This work was performed with the support and under the auspices of the NIFS Collaboration Research Programs (NIFS09KUTR046/NIFS10KUTR048 /NIFS11KUTR059/NIFS11KUTR069). This research was partially supported by the Ministry of Education, Science, Sports and Culture, Grant-in-Aid for Sc. Res. (B) [21360452].

[1] K. Hanada *et al.*, Proc. of the 22nd IAEA Fusion Energy Conference (2008), FT/P3-25.
[2] A. Fukuyama, Fusion Eng. Design **53**, 71 (2001).
[3] H. Idei *et al.*, J. Plasma Fusion Res. Series **8**, 1104 (2009).
[4] E. Kalinnikova *et al.*, IEEJ Trans. FM, **132**, 505 (2012).
[5] H. Idei *et al.*, Proc. of the Joint 32nd International Conference on Infrared and Millimetre Waves and 15th International Conference on Terahertz Electronics (2007).
[6] H. Idei *et al.*, Proc. of the Joint 34th International Conference on Infrared and Millimetre Waves and 17th International Conference on Terahertz Electronics (2009).
[7] H. Idei *et al.*, Proc. of the 23rd IAEA Fusion Energy Conference (2010), EXW/P7-31.
[8] H. Idei *et al.*, Nucl. Fusion **46**, 489 (2006).
[9] K.L. Wong *et al.*, Phys. Rev. Lett. **45**, 117 (1980).
[10] H. Zushi *et al.*, submitted to Phys. Rev. Lett.